High-Resolution Silicon-29 Nuclear Magnetic Resonance in the Y-Si-O-N System

R. Dupree,* M. H. Lewis, and M. E. Smith

Contribution from the Department of Physics, University of Warwick, Coventry CV4 7AL, U.K.
Received July 10, 1987

Abstract: The isotropic ^{29}Si chemical shifts for the complete range of mixed tetrahedral coordinations SiO_xN_{4-x} ($0 \le x \le 4$) have been obtained by using the crystalline phases of the Y-Si-O-N system. Although some overlap of the chemical shift ranges from different tetrahedral units occurs, it is normally possible to differentiate distinct environments, allowing refinement of structural data and providing information on phase evolution in oxynitride systems. As an example, the most likely atomic arrangement for *N*-melilite ($Y_2Si_3O_3N_4$) has been determined by using these shift ranges.

In the 7 years since the first high-resolution solid-state ^{29}Si NMR spectra from inorganic materials were obtained[1] there have been an increasing number of applications of this technique. The local electronic environment of a nucleus subtly influences the NMR frequency, and it is this effect that makes NMR a sensitive probe of the local structure of a material. The technique of magic-angle spinning (MAS)[2] is widely employed to remove anisotropic broadening (e.g., dipolar, chemical shift), which would otherwise mask the small changes of the isotropic chemical shift in solids. ^{29}Si MAS NMR has been carried out on a number of crystalline materials, including minerals,[3,4] zeolites,[5] and phyllosilicates[6] as well as amorphous materials.[7-9] In many of these materials conventional X-ray diffraction (XRD) techniques can provide little detailed information about the local structure since either the X-ray scattering factors of the constituent elements are very similar (e.g., silicon and aluminum in aluminosilicates) or there is no long-range order, which leads to diffuse, featureless XRD patterns.

The ^{29}Si chemical shifts in silicates depend on a number of structural factors, the most important being the local coordination, with SiO_4 tetrahedra resonating between -60 and -130 ppm[10,11] (with respect to tetramethylsilane (TMS)) while SiO_6 octahedra resonate between -180 and -220 ppm.[12] For SiO_4 tetrahedra the chemical shifts of the resonance frequency have been attributed to a number of factors, including connectivity, next-nearest-neighbor, cation type, and bond length and angle.[3,10,11] Even very subtle structural differences can be observed in crystalline materials such as δ-$Y_2Si_2O_7$, where the two silicons of the $Si_2O_7^{6-}$ group have slight differences of 0.6% in the terminal silicon-oxygen bond lengths, leading to a distinct splitting of the resonance of $\sim$1.7 ppm.[13,14]

A common feature of all these studies is that silicon is directly bonded only to oxygen. Recently, the range of silicon tetrahedra has been expanded to include SiO_xN_{4-x} ($0 \le x \le 4$) by the study of some sialon ceramic phases[15,16] and some yttrium sialon glasses.[17] The crystalline phases studied include α-Si_3N_4, β-Si_3N_4, Si_2N_2O, β'-sialon, and some polytypoids. These spectra have provided useful information about the local silicon coordination in these materials, particularly for β'-sialon, which was not previously available. The general trend of the ^{29}Si chemical shift to higher frequencies (-63 ppm for Si_2N_2O ($SiON_3$) and -49 ppm for β-Si_3N_4 (SiN_4)) with increasing nitrogen content may be related to the decrease in electronegativity of the elements bonded to the silicon. Small inequivalences in the SiN_4 tetrahedra in α-Si_3N_4 are readily detected.[15] The ^{29}Si spectra of the Y-Si-Al-O-N glasses show a similar trend in the shifts of these tetrahedra although the shifts were obtained from Gaussian fits to broad lines as the different environments could not be completely resolved.

This study extends the range of these tetrahedra that have been observed by MAS NMR in crystalline solids by examining the crystalline phases of the Y-Si-O-N system (Figure 1). Some of these phases form as crystallization products in some technologically important Y-Si-Al-O-N ceramics.[18] The structure of many of these phases is not well-known, and in this paper it will be demonstrated that high-resolution solid-state NMR can aid structural refinement as well as monitoring phase development.

Table I. Summary of the Isotopic Silicon Chemical Shifts, Line Width (FWHM), and Tetrahedral Units of Y-Si-O-N Phases

phase	proposed silicon structural tetrahedron	chem shift[a]	FWHM[b]
β-Si_3N_4	SiN_4-$Q^{(8)}$	-49.0	120
Si_2N_2O	SiN_3O-$Q^{(7)}$	-63.0	200[c]
γ-$Y_2Si_2O_7$	SiO_4-$Q^{(1)}$	-92.8	$\sim$50
Y_2SiO_5	SiO_4-$Q^{(0)}$	-79.8	80
N-apatite ($Y_5Si_3O_{12}N$)	SiO_4-$Q^{(0)}$	-74.8	210
	SiO_3N-$Q^{(0)}$	-67.5	250
N-YAM ($Y_4Si_2O_7N_2$)	SiO_3N-$Q^{(1)}$	-74.4	320
N-wollastonite ($YSiO_2N$)	SiO_2N_2-$Q^{(2)}$	-65.3	400
N-melilite ($Y_2Si_3O_3N_4$)	SiO_2N_2-$Q^{(3)}$,$Q^{(4)}$	-56.7	430
YSi_3N_5	SiN_4	-45.5	140
		-42.3	

[a] In ppm; with respect to δ(TMS) = 0 ppm; $\pm$0.5 ppm. [b] In hertz; $\pm$30 Hz. [c] Taken from ref 15.

Experimental Section

The crystalline phases were prepared by solid-state sintering of stoichiometric mixtures of pure (>99.9%) Y_2O_3, SiO_2, and Si_3N_4 powders. These powders were dry mixed followed by compaction into pellets, which

(1) Lippmaa, E.; Magi, M.; Samosen, A.; Engelhardt, G.; Grimmer, A.-R. *J. Am. Chem. Soc.* **1980**, *102*, 4889-4893.
(2) Andrew, E. R. *Int. Rev. Phys. Chem.* **1981**, *1*, 195-229.
(3) Smith, K. A.; Kirkpatrick, R. J.; Oldfield, E.; Henderson, D. M. *Am. Mineral.* **1983**, *68*, 1206-1215.
(4) Fyfe, C. A.; Gobbi, G. C.; Putnis, A. *J. Am. Chem. Soc.* **1986**, *108*, 3218-3223.
(5) Klinowski, J. *Prog. NMR Spectrosc.* **1984**, *16*, 237-309.
(6) Sanz, J.; Serratosa, J. M. *J. Am. Chem. Soc.* **1984**, *106*, 4790-4793.
(7) Dupree, R.; Pettifer, R. *Nature (London)* **1984**, *308*, 523-524.
(8) Dupree, R.; Holland, D.; McMillan, P. W.; Pettifer, R. *J. Non-Cryst. Solids* **1984**, *68*, 399-410.
(9) Schramm, C. M.; de Jong, B. H. W. S.; Parziale, V. E. *J. Am. Chem. Soc.* **1984**, *106*, 4396-4402.
(10) Magi, M.; Lippmaa, E.; Samosen, A.; Engelhardt, G.; Grimmer, A.-R. *J. Phys. Chem.* **1984**, *88*, 1518-1522.
(11) Janes, N.; Oldfield, E. *J. Am. Chem. Soc.* **1985**, *107*, 6769-6775.
(12) Grimmer, A.-R.; Von-Lampe, F.; Magi, M.; *Chem. Phys. Lett.* **1986**, *132*, 549-553.
(13) Grimmer, A.-R.; Von-Lampe, F.; Magi, M.; Lippmaa, E. *Monatsh. Chem.* **1984**, *115*, 561-564.
(14) Leng-Ward, G.; Smith, M. E., unpublished results.
(15) Dupree, R.; Lewis, M. H.; Leng-Ward, G.; Williams, D. S. *J. Mater. Sci. Lett.* **1985**, *4*, 393-395.
(16) Klinowski, J.; Thomas, J. M.; Thompson, D. P.; Jack, K. H.; Fyfe, C. A.; Gobbi, G. C. *Polyhedron* **1984**, *11*, 1267-1271.
(17) Aujla, R. S.; Leng-Ward, G.; Lewis, M. H.; Seymour, E. F. W.; Styles, G. A.; West, G. W. *Philos. Mag. Lett.* **1986**, *54*, 51-56.
(18) Jack, K. H. *J. Mater. Sci.* **1976**, 1135-1158.

0002-7863/88/1510-1083$01.50/0

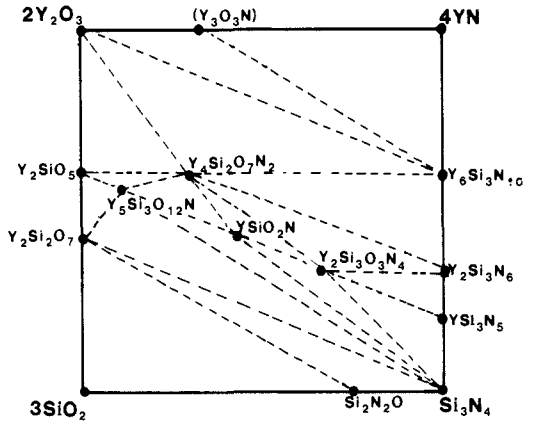

Figure 1. Crystalline phases of the Y–Si–O–N system (after ref 20).

were embedded in BN in a graphite crucible. The samples were heated to 1550–1700 °C in an graphite-susceptor induction furnace for ~2 h under a flowing oxygen-free nitrogen atmosphere. All samples were checked for mass loss and no significant effects were found (<2%). The products were characterized by conventional X-ray diffraction (XRD) and scanning electron microscopy (SEM).

The MAS NMR was performed on a Bruker MSL-360 spectrometer operating at 71.535 MHz for ^{29}Si. All spectra were accumulated by using small pulse angles (10–15°) and 60-s pulse delays for ~800 scans. A problem with these samples is that some phases have very long spin–lattice relaxation times (T_1 on the order of hours). Conditions were chosen to maximize signal-to-noise so that the chemical shifts could be obtained, but it should be remembered that accurate quantitative data on the phase distribution may be lost due to differential saturation. The samples were finely powdered and packed into conventional "mushroom" spinners which held ~0.5 g of sample and were spun at 3–3.5 kHz. Data processing involved application of 0–100-Hz exponential smoothing to improve the signal-to-noise. All spectra were referenced to an external TMS standard.

NMR Data

The results of our high-resolution ^{29}Si NMR experiments on the crystalline phases of the Y–Si–O–N system are summarized in Table I, which includes the isotropic chemical shifts, FWHM, and proposed structural units for these compounds. For conclusive identification of the isotropic shifts from particular phases it is desirable to produce single-phase products. When this is not possible, the peaks may be attributed to particular phases by correlating the changing levels of the phases present after different heat treatments as indicated by XRD with the changes of intensity of the NMR peaks.

Single-phase γ-$Y_2Si_2O_7$ (Ito et al. nomenclature[19]) was produced by annealing a sample that had initially been fired at 1700 °C for 2 h at 1400 °C (Figure 2a). A single-phase product of the high-temperature polymorph Y_2SiO_5 (Figure 2b) and *N*-YAM ($Y_4Si_2O_7N_2$) (Figure 2c) were also produced. *N*-Wollastonite ($YSiO_2N$) proved more difficult to form as it decomposes above 1400 °C, with all sinterings producing mixtures of $Y_4Si_2O_7N_2$, $YSiO_2N$, and Si_3N_4. At higher temperatures more *N*-YAM forms while at lower temperatures the reaction kinetics become very sluggish. The most single-phase *N*-wollastonite (figure 2d) produces three resonances, which are assigned to Si_3N_4 (–49 ppm), $YSiO_2N$ (–65.3 ppm), and $Y_4Si_2O_4N_2$ (–74.4 ppm), and this is confirmed by XRD and SEM analysis. Sinterings at the *N*-apatite composition also form multiphase products (Figure 3a,b). XRD identifies four phases, *N*-apatite, Y_2SiO_5, together with small amounts of *N*-YAM, and unreacted yttria. The MAS NMR peaks at –67.5 and –74.8 ppm are tentatively assigned to *N*-apatite, with the peak at –79.8 ppm corresponding to Y_2SiO_5. The changes in amplitude of these peaks agree with the changes of phase content of these samples determined by XRD. Holding an *N*-apatite-containing specimen in an oxygen atmosphere (Figure 3c) results in the amount of *N*-apatite being much reduced while there is an increase in the level of Y_2SiO_5.

The most intriguing phase of all in this system has proved to be *N*-melilite, and Figure 4 shows the general phase development with changing heat treatment. The NMR spectra and XRD patterns initially proved difficult to interpret. The initial stages of reaction (Figure 4a,b) have large amounts of unreacted Si_3N_4

(19) Ito, J.; Johnson, H. *Am. Mineral.* **1968**, *53*, 1940–1952.

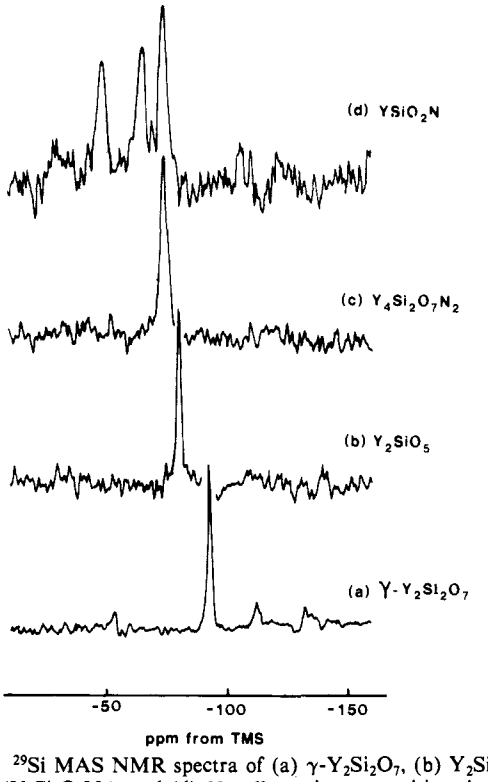

Figure 2. ^{29}Si MAS NMR spectra of (a) γ-$Y_2Si_2O_7$, (b) Y_2SiO_5, (c) *N*-YAM ($Y_4Si_2O_7N_2$), and (d) *N*-wollastonite composition sintered at 1550 °C for 2 h.

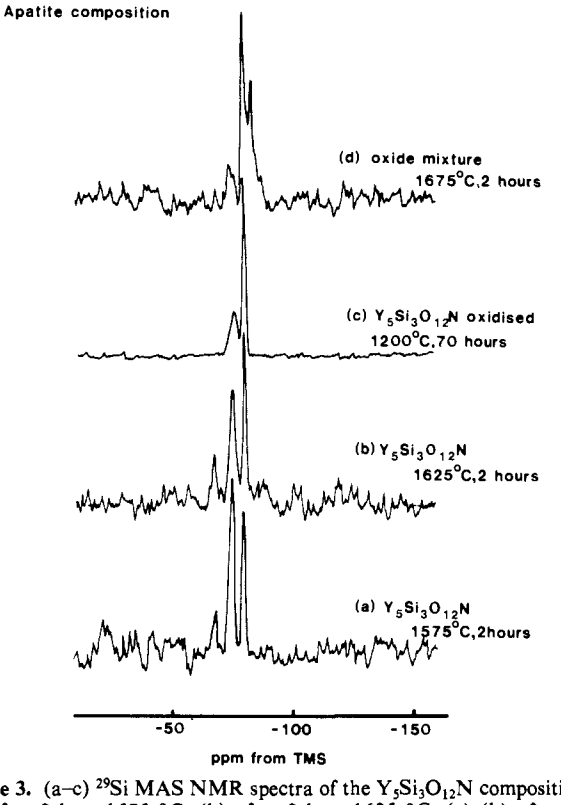

Figure 3. (a–c) ^{29}Si MAS NMR spectra of the $Y_5Si_3O_{12}N$ composition: (a) after 2 h at 1575 °C; (b) after 2 h at 1625 °C; (c) (b) after an additional 70 h at 1200 °C in an oxygen atmosphere. (d) ^{29}Si MAS NMR spectrum of an apatite stoichiometric mixture of Y_2O_3 and SiO_2 after 1675 °C for 2 h.

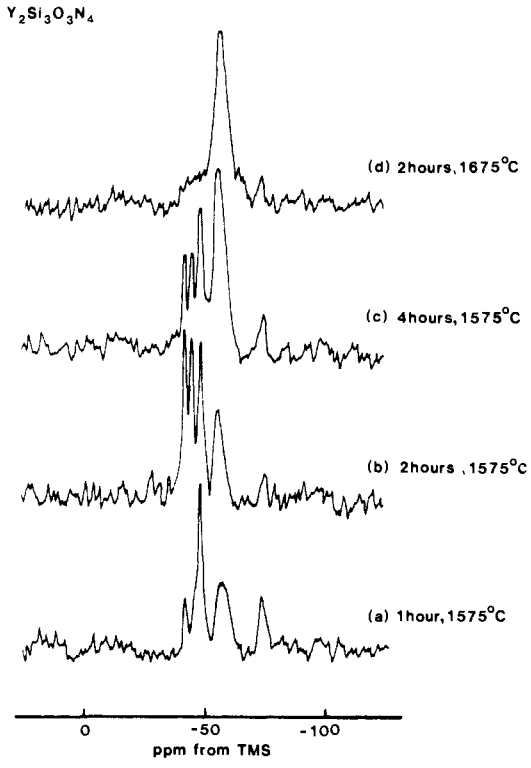

Figure 4. ^{29}Si MAS NMR spectra of $Y_2Si_3O_3N_4$ after various heat treatments.

(−49 ppm) together with some *N*-melilite (−56.7 ppm), small amounts of *N*-YAM (−74.4 ppm), and another phase corresponding to the peaks at −42.3 and −45.5 ppm. The presence of *N*-YAM can be explained as reactions with Si_3N_4 usually involve some SiO_2 which forms as a surface oxidation layer, and it has already been shown that *N*-YAM readily forms at 1550 °C. Both peaks at −42.3 and −45.5 ppm increase with additional heat treatment before completely disappearing when almost single-phase *N*-melilite is produced (Figure 4d). Although the XRD patterns from the initial heat treatment were complex due to the multiphase nature of the specimens, a broad, weak XRD peak with a *d* spacing of −2.73 Å can be correlated with the MAS NMR peaks at −42.3 and −45.5 ppm since when *N*-melilite is absent (Figure 5b) this XRD peak becomes intense. A recent publication[20] has identified three phases along the YN–Si_3N_4 tie line, and this XRD peak may be attributed to the hexagonal phase YSi_3N_5. The formation of YSi_3N_5 agrees with the behavior diagram for this system (Figure 1).

The results of nominally similar heat treatments on the *N*-melilite composition can produce markedly different results (Figures 4a and 5a and Figures 4b and 5b) unlike the other compositions, which are readily reproducible. Figure 5d is the result of sintering an *N*-melilite composition with 5 mol % excess silica at 1575 °C for 2 h. The reaction kinetics have clearly been speeded up by the addition of silica, probably due to the formation of a eutectic sintering liquid at this oxygen-rich melilite composition.

It should be emphasized that as some of these phases have very long relaxation times ($T_1 > 2$ h), the spectra do not give a true reflection of the phase distribution. Figures 4c and 5c are of the same sample, except the delay is much longer for the latter (1 min for Figure 4c; 20 min for Figure 5c). The Si_3N_4 and *N*-melilite peaks increase in intensity relative to those from YSi_3N_5. Although most of these spectra are partially saturated, they are still useful for obtaining the isotropic chemical shift, and, provided the conditions are kept constant, any relative change of peak intensities (Figure 3a,b) reflects the relative changes in the phase content.

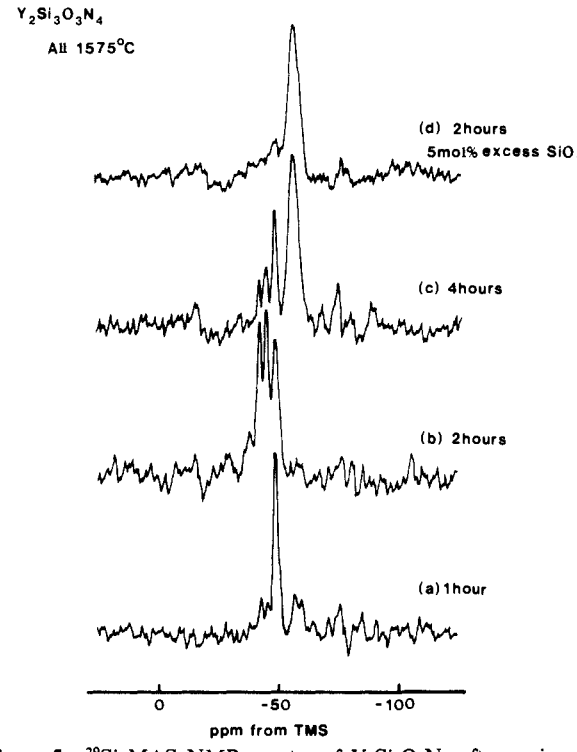

Figure 5. ^{29}Si MAS NMR spectra of $Y_2Si_3O_3N_4$ after various heat treatments. (c) The same sample as in Figure 4c (1-min pulse delay) with a 20-min pulse delay. (d) *N*-melilite composition made up with 5 mol % excess silica.

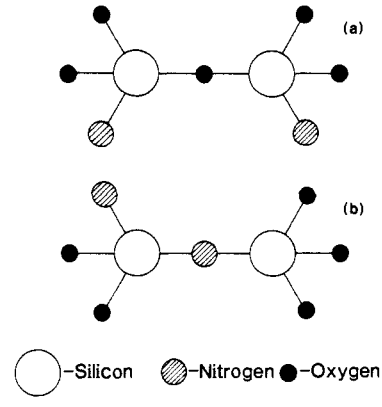

Figure 6. Possible atomic arrangements of the $Si_2O_5N_2$ group of *N*-YAM ($Y_4Si_2O_7N_2$).

Discussion

In the Y_2O_3–SiO_2 system two silicates are known to form, $Y_2Si_2O_7$, which has at least four polymorphs, and Y_2SiO_5, which has two. NMR data for the δ- and γ-$Y_2Si_2O_7$ polymorphs[13] are the only previous measurements of shifts in this system, with the value for this study, −92.8 ppm, for γ-$Y_2Si_2O_7$ being in agreement with that work. The surprisingly negative shift for this SiO_4-$Q^{(1)}$ unit (where $Q^{(n)}$ indicates an SiO_xN_{4-x} tetrahedron connected to *n* other tetrahedra) may be explained by the Si–O–Si bond angle being 180°. Since the oxygen's orbital electronegativity increases with increasing bond angle, for a particular Q type the shift will be most negative when the bond angle is 180°. The shift of −79.8 ppm for the high-temperature Y_2SiO_5 polymorph is consistent with isolated SiO_4-$Q^{(0)}$ tetrahedra. The trends in the ^{29}Si chemical shift for SiO_4-containing materials are reasonably well understood. For a series of materials, when factors such as cation type are held constant, the resonance shifts to lower frequency with increasing *n*. This may be explained in terms of changes in the degree of covalency of the Si–O bonds, with the average covalency of these

(20) Thompson, D. P. In *Tailoring Multiphase and Composite Ceramics*; Tressler, R. E., Messing, G. L., Pantano, C. G., Newnham, R. G., Eds.; Plenum: New York, 1986; pp 79–91.

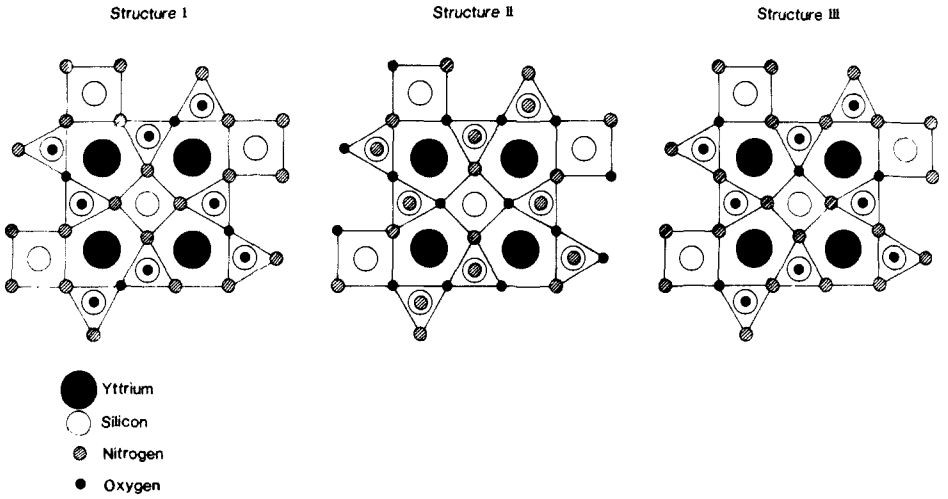

Figure 7. Possible atomic arrangements of $Y_2Si_3O_3N_4$ under the sole constraint of stoichiometry.

bonds decreasing with increasing polymerization, leading to smaller paramagnetic shifts (i.e., toward lower frequency). Although this general trend is followed by SiO_4 units, there exists considerable overlap of the shift ranges associated with each Q type due to the many other influences on the chemical shift.

The $Y_4Si_2O_7N_2$ phase is isostructural with the mineral cuspidine ($Ca_4Si_2O_7F_2$), and it is of interest whether the nitrogen bonds to silicon or whether it replaces fluorine. Crystal chemistry arguments using Pauling's second crystal rule (PSCR) (which is essentially a local charge/bond strength balancing rule)[21] suggest that nitrogen bonds to silicon.[22] Two possible arrangements of the $Si_2O_5N_2$ unit are shown in Figure 6. The MAS NMR spectrum (Figure 2c) shows a single resonance at −74.4 ppm. This is consistent with Figure 6a, which only has SiO_3N tetrahedra, and is in agreement with a neutron diffraction study.[23] The only other possibility (Figure 6b) has both SiO_2N_2 and SiO_3N tetrahedra, which would be expected to produce two distinct resonances.

The *N*-wollastonite resonance at −65.3 ppm provides a useful standard since the crystal structure of this phase has been fully determined.[24] This provides a well-defined structural unit consisting of a ring of three SiO_2N_2 tetrahedra with each tetrahedron connected via nitrogen to the other two tetrahedra. This gives a shift for a SiO_2N_2-$Q^{(2)}$ tetrahedron of −65.3 ppm. The resonance peak line widths (FWHM), which are significantly broader for these oxynitrides compared to most silicates, can aid spectral interpretation. The increased widths can be attributed to local variations in environment and also the fact that the silicon is bonded to ^{14}N, a quadrupolar nucleus. MAS averaging of the dipolar coupling between silicon and nitrogen is significantly impaired when the quadrupole interaction of the nitrogen is sufficiently large (quadrupole interaction/Zeeman interaction >0.2).[25] Assuming these factors are comparable for *N*-wollastonite and *N*-YAM, their similar widths (Table I) suggest a single silicon environment in *N*-YAM.

N-Apatite is thought to exist over a range of compositions $Y_5(SiO_3N)_3\square$ (□ = vacancy)–$Y_5Si_3O_{12}N$. It has been suggested that this solid solution may extend to the Y_2O_3–SiO_2 tie line with a silicate phase of approximate composition $Y_{\sim 4.67}(SiO_4)_3O$–$Y_4Si_3O_{12}$. By direct sintering of the oxides in this composition range at 1675 °C mixtures of only $Y_2Si_2O_7$ and Y_2SiO_5 resulted (Figure 3d), in agreement with a previous XRD study.[26] Oxidation of *N*-apatite at 1200 °C also gives no evidence of a purely oxygen-containing phase, which indicates that the nitrogen is important in stabilizing this structure. For *N*-apatite application of PSCR indicates that any nitrogen in this structure should be directly bonded to silicon; hence the resonance of −67.3 ppm is assigned to SiO_3N-$Q^{(0)}$ and that at −74.8 ppm is attributed to SiO_4-$Q^{(0)}$.

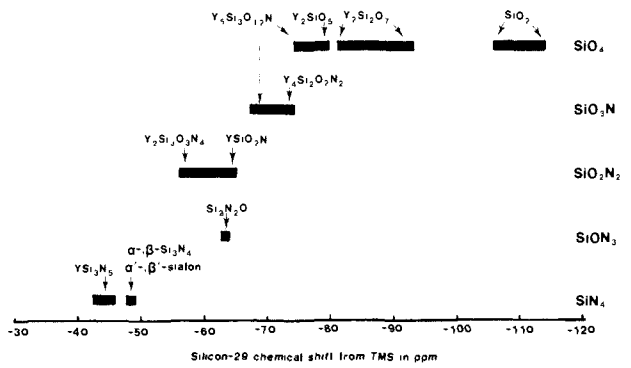

Figure 8. ^{29}Si chemical shifts of SiO_xN_{4-x} ($0 \leq x \leq 4$) tetrahedra from crystalline ceramic phases.

The atomic arrangement of *N*-melilite is not known. As this phase is isostructural with the mineral melilite, it is known to consist of sheets of SiO_xN_{4-x} tetrahedra with yttrium ions between the layers. Figure 7 shows three possible atomic arrangements of this structure consistent with the sole constraint of the overall stoichiometry, $Y_2Si_3O_3N_4$. According to a previous neutron diffraction study of this phase,[23] structure I is favored, with the $Si_2O_3N_4$ grouping arranged as two SiO_2N_2 tetrahedra with the third silicon in an SiN_4 environment. The other two possibilities in Figure 7 have different local silicon tetrahedra, with structure III consisting of $SiON_3$ and SiO_2N_2 tetrahedra, while structure II has just one type of tetrahedra, SiO_2N_2. Although XRD shows the products formed during the early stages of reaction principally to be *N*-melilite, the MAS NMR spectra (Figure 4b,c) indicate both mixed oxygen/nitrogen tetrahedra (−56.7 ppm) and SiN_4 tetrahedra (−42.3 and −45.5 ppm). The SiN_4 units have been assigned to YSi_3N_5, with only the −56.7 ppm peak associated with *N*-melilite, which is confirmed by the single peak produced after higher temperature reaction (Figure 4d). These MAS NMR results favor structure II since two distinct tetrahedral coordinations would be expected to produce two resonances. The more subtle distinction of Q type would be expected to produce a smaller chemical shift dispersion, which in this case cannot be resolved but accounts for the relatively large line width of *N*-melilite.

The YSi_3N_5 phase has two resonances, which indicates two inequivalent silicon sites. Their position, more positive than silicon nitride, are consistent with SiN_4 tetrahedra, with some of the bonds being nonbridging (i.e., $Y^+\cdots{}^-N$). In the lanthanum compound

(21) McKie, D.; McKie, C. In *Crystalline Solids*; Nelson, Ed.; 1974; pp 324–326.
(22) Morgan, P. E. D. *J. Mater. Sci. Lett.* **1986**, *5*, 372.
(23) Roult, R.; Bacher, P.; Liebaut, G.; Marchand, R.; Goursat, P.; Laurent, Y. *Acta Crystallogr., Sect. A* **1984**, *A40* (*Suppl.*), C226.
(24) Morgan, P. E. D.; Carroll, P. J.; Lange, F. F. *Mater. Res. Bull.* **1981**, *12*, 251–259.
(25) Bohm, J.; Fenzke, D.; Pfeifer, H. *J. Magn. Reson.* **1983**, 197–204.
(26) Liddell, K.; Thompson, D. P. *Br. Ceram. Trans. J.* **1986**, *85*, 17–22.

$LaSi_3N_5$, which has had its crystal structure determined,[27] such SiN_4 tetrahedra are present. This is the first observation of nonbridging SiN_4 tetrahedra by solid-state NMR.

The shift ranges summarized in Figure 8 show a general trend to more positive chemical shifts with increasing nitrogen coordination of silicon, consistent with the changing covalency of the bonds. As the Si–N bond is more covalent than the Si–O bond, the replacement of oxygen by nitrogen increases the average bond covalency, leading to a deshielding of the silicon, making the chemical shift of each successive $SiO_{4-x}N_x$ (increasing x) more positive. However, from the shifts presented here it can be seen that there is no strict ordering of the shifts, with the SiO_2N_2-$Q^{(2)}$ in $YSiO_2N$ at a more negative chemical shift than SiO_2N_2-$Q^{(3)}Q^{(4)}$ in $Y_2Si_3O_3N_4$. However, as for previous studies on silicates, there can be expected to be an extensive overlap of the shift ranges of the different structural units, reflecting the fact that the NMR chemical shift is an involved function of the structure. In other, mainly solution-state studies of SiX_aY_b ($a + b = 4$) tetrahedra, the chemical shift rarely follows a linear variation with some intermediate member having the largest p-electron imbalance about the silicon and thus having the most paramagnetic shift.[28] It is quite likely therefore that the chemical shift difference between successive SiO_xN_{4-x} tetrahedra is nonlinear (and possibly not monotonic), enhancing the overlap of the chemical shift ranges.

(27) Inoue, Z.; Mamoru, M. *J. Mater. Sci.* **1980**, *15*, 2915–2920.
(28) Tossell, J. A.; Lazzeretti, P. *Chem. Phys. Lett.* **1986**, *133*, 463–465.

Conclusion

The chemical shifts for all tetrahedra SiO_xN_{4-x} ($0 \le x \le 4$) can now be given from the MAS NMR spectra of the Y–Si–O–N crystalline phases. The general trend to more positive chemical shifts with increasing nitrogen may be attributed to the greater covalency of the bonds. The extensive overlap of the chemical shifts of different tetrahedral units means that no resonance can be unambiguously assigned to a given unit (as with silicates) if no other information is available. MAS NMR can be used in exactly the same manner as XRD to identify phases once a catalog of chemical shifts has been established. This has been demonstrated for *N*-apatite and *N*-melilite with the additional advantage that the spectra can be made truly quantitative. The sensitivity of the chemical shift to the local environment is a useful aid to structural studies of these phases. This has allowed us to refine the structures of *N*-YAM and *N*-melilite. To obtain a better understanding of the influences on the ^{29}Si chemical shift in the solid state the range of compounds studied containing SiO_xN_{4-x} tetrahedra will have to be further expanded.

Acknowledgment. We thank the SERC for support and a studentship (M.E.S.).

Registry No. Y, 7440-65-5; Si, 7440-21-3; O_2, 7782-44-7; N_2, 7727-37-9; $Y_2Si_3O_3N_4$, 54650-98-5; $Y_2Si_2O_7$, 14286-95-4; Y_2SiO_5, 12027-88-2; $Y_4Si_2O_7N_2$, 58694-26-1; $YSiO_2N$, 62361-78-8; Si_3N_4, 12033-89-5; Si_2N_2O, 12033-76-0; $Y_5Si_3O_{12}N$, 59977-54-7; YSi_3N_5, 112068-60-7.

Equilibrium Isotope Effects on the Hydration of Gas-Phase Ions. The Effect of Hydrogen Bond Formation on Deuterium Isotopic Fractionation Factors for H_3O^+, $H_5O_2^+$, $F(H_2O)^-$, and $Cl(H_2O)^-$

J. W. Larson and T. B. McMahon*

Contribution from the Department of Chemistry and Guelph-Waterloo Centre for Graduate Work in Chemistry, University of Waterloo, Waterloo, Ontario, Canada N2L 3G1.
Received May 4, 1987

Abstract: Equilibrium isotope exchange reactions have been examined for transfer of $H^+(D^+)$, $H_3O^+(H_2OD^+, HOD_2^+, D_3O^+)$, F^-, and Cl^- among H_2O, HOD, and D_2O. In each case ions are found to be more favorably coordinated to H_2O rather than D_2O. These results are compared to similar data for ions in H_2O or D_2O solution. Statistical thermodynamic arguments are presented which imply that rotational effects play an important role in determination of the overall isotope effect, in addition to the more commonly considered zero-point energy effects. The important role of the inversion mode of H_3O^+ on the isotope effect is considered. Implications for isotope fractionation in the interstellar medium are discussed.

The examination of solvent isotope effects has been used extensively as a probe of the nature of hydrogen-bonded interactions between solute and solvent species.[1] In some situations the general observation has been made that interactions of strong acids with solvent favor deuterium bonds, while weak acids interact preferentially via hydrogen bonds.[2] This statement, while appearing to be borne out by limited experimental data, has not been explained fully on a rational physical basis.

It has been shown recently from studies of gas-phase hydronium ion in this laboratory[3] that the claim that in general hydrogen will accumulate in species where the site of isotopic substitution is in the lower force field appears to be true. This result was attributed to be a direct consequence of a greater zero-point energy difference between H_3O^+ and D_3O^+ relative to that between H_2O and D_2O. However, in another study of isotopic fractionation in the ClH-Cl^-–$ClDCl^-$ system[4] it was shown that, particularly for small ions, differences in rotational partition functions due to significant differences in moments of inertia can dominate the isotope effect. This effect was shown to reinforce that of the vibrational zero-point

(1) (a) Kreevoy, M. M. In *Isotope Effects in Organic Chemistry*; Buncel, E., Lee, C. C., Eds.; Elsevier: Amsterdam, 1976; Vol. 2. (b) More O'Ferrall, R. A. In *Proton Transfer Reactions*; Caldin, E. C., Gold, V., Eds.; Chapman and Hall: London, 1975. (c) Schowen, R. L. *Prog. Phys. Org. Chem.* **1972**, *9*, 275. (d) Schowen, R. L. In *Isotope Effects on Enzyme Catalyzed Reactions*; Cleland, W. N., O'Leary, M. H., Northrup, D. B., Eds.; University Parke Press: Baltimore, MD, 1977. (e) Lias, S. G. *J. Phys. Chem.* **1984**, *88*, 4401.
(2) Joesten, M. D.; Schaad, L. J. *Hydrogen Bonding*; Marcel-Dekker: New York, 1974.
(3) Larson, J. W.; McMahon, T. B. *J. Am. Chem. Soc.* **1986**, *108*, 1719.

0002-7863/88/1510-1087$01.50/0